

DETERMINATION OF DISPERSION CURVES FOR COMPOSITE MATERIALS WITH THE USE OF STIFFNESS MATRIX METHOD

Marek BARSKI*, Piotr PAJAŁ*

*Institute of Machine Design, Faculty of Mechanical Engineering, Cracow University of Technology,
al. Jana Pawła II 37, 31-864, Kraków, Poland

mbar@mech.pk.edu.pl, ppajak@mech.pk.edu.pl

received 10 October 2016, revised 11 May 2017, accepted 15 May 2017

Abstract: Elastic waves used in Structural Health Monitoring systems have strongly dispersive character. Therefore it is necessary to determine the appropriate dispersion curves in order to proper interpretation of a received dynamic response of an analyzed structure. The shape of dispersion curves as well as number of wave modes depends on mechanical properties of layers and frequency of an excited signal. In the current work, the relatively new approach is utilized, namely stiffness matrix method. In contrast to transfer matrix method or global matrix method, this algorithm is considered as numerically unconditionally stable and as effective as transfer matrix approach. However, it will be demonstrated that in the case of hybrid composites, where mechanical properties of particular layers differ significantly, obtaining results could be difficult. The theoretical relationships are presented for the composite plate of arbitrary stacking sequence and arbitrary direction of elastic waves propagation. As a numerical example, the dispersion curves are estimated for the lamina, which is made of carbon fibers and epoxy resin. It is assumed that elastic waves travel in the parallel, perpendicular and arbitrary direction to the fibers in lamina. Next, the dispersion curves are determined for the following laminate $[0^\circ, 90^\circ, 0^\circ, 90^\circ, 0^\circ, 90^\circ, 0^\circ, 90^\circ]$ and hybrid $[Al, 90^\circ, 0^\circ, 90^\circ, 0^\circ, 90^\circ, 0^\circ]$, where Al is the aluminum alloy PA38 and the rest of layers are made of carbon fibers and epoxy resin.

Key words: Structural Health Monitoring, Layered Composite Materials, Guided Waves, Dispersion Curves, Stiffness Matrix Method

1. INTRODUCTION

Nowadays layered composite materials are widely used in different structures. This is particularly evident in the aerospace industry. The main advantage of using composite materials is the fact that structures are substantially lighter in comparison with structures made of traditional isotropic materials, like steel or aluminum alloys. On the other hand, process of damage formation and evaluation in composite materials is much more complex. In order to detect the different kind of flaws (matrix cracking, fiber breakage or delamination), sophisticated methods have to be applied. Some of them are based on an analysis of propagation of elastic waves, which travel through the investigated structure (Giurgiutiu, 2008). Generally, this kind of systems can be applied in two different configurations, namely pitch-catch and pulse-echo. First approach is based on the comparison of received signals for intact and interrogated structure. In the case when the signals are different, it means that inside the material there is a damage. It is worth stressing here that without the knowledge about an intact structure, the damage detection is impossible. This is the main disadvantage of this approach. The latter method is based on an analysis of received reflection of elastic waves from a flaw. Thus this approach can be utilized in the case when the dynamic response of an intact structure is unknown. However, elastic waves have strongly dispersive nature (Royer and Dieulesaint, 2000). Moreover, depending on the frequency of the excitation signal, the different number of wave modes are present. Therefore, for appropriate interpretation of a picked up dynamic response of the structure, the dispersion curves have to be determined. However, it could be a very difficult task in the case of composite structure.

One of the first approach, known as the transfer matrix method was proposed by Thompson (1950). He introduced so called transfer matrix, which relates the displacement and stress at the top and bottom of the layer. The matrices for any number of isotropic layers could be coupled into one. This approach was further corrected by Haskell (1953). Originally, this approach is limited to the materials where all layers are made of isotropic materials. Nayfeh (1991;1995) extended this method to the case, where layers are made of anisotropic materials. The transfer matrix method is relatively simple and easy to use. The first computer applications based on this algorithm were developed in the sixties of the last century (Press et al., 1961; Randall, 1967). However, this method is numerically unstable in the case of relatively high frequencies as well as thicker layers. This problem is well known in literature as "fd problem" (Lowe, 1995). An alternative to the transfer matrix algorithm is the global matrix method proposed by Knopoff (1964). In this approach the dynamic properties of a whole composite material are described by single matrix (global matrix). The size of this matrix directly depends on the number of layers. Besides, the fd problem is still present in this formulation. Initially, this method was applied in the case of isotropic layers (Schwab 1970; Schmidt and Tango, 1986). Nowadays, the global matrix method is also applied in the case of composites, which consist of anisotropic layers (Pant et al., 2014). There is also available a commercial program DISPERSE (Pavlovic and Lowe, 2003), which is based on this approach. The third analytical method of dispersion curves determination was proposed by Kausel (1986) and further developed by Wang and Rokhlin (2001; 2002a; 2002b). It is known as the stiffness matrix method. According to its authors, this method is numerically unconditionally stable. The mentioned above transfer matrix is replaced by a layer

stiffness matrix, which relates the stresses at the top and the bottom of the layer with the displacement at the top and bottom of the layer. Next, the global stiffness matrix for the whole composite material is obtained by the use of an effective, recursive algorithm. It is worth stressing here that the numerical stability is achieved by replacing the exponential terms from the diagonal of the stiffness matrix. Besides, this approach has the same dimension and is only slightly more computationally efficient in comparison with the transfer matrix method (Giurgiutiu, 2008). This approach is used by Kamal and Giurgiutiu (2014) in case of the multilayered anisotropic composites. The authors also verify the stiffness matrix method with the use of the transfer matrix method, program DISPRESSE and the semi-analytical finite element method (Soro-han et al., 2011). It seems that nowadays the stiffness matrix method is the most effective analytical method, which enables the dispersion curves determination. However, in the case of composites, where there is a significant difference between the stiffness of the particular layer or there are strongly orthotropic layers, the numerical problems may be still present. Therefore, the main aim of this work is to estimate the dispersion curves for the composites, which consist of this kind of layer materials, namely fibers with epoxy resin (CFRP, Fibers T300, Matrix N5208) and aluminum alloy PA38. Moreover, the present work should be considered as the continuation of the previous studies (Barski and Pająk, 2016). In that paper the dispersion curves obtained for a single lamina and for a multilayered composite material with quasi - isotropic mechanical properties are presented. The computations were made for the glass fibers GFRP E-glass and epoxy resin.

2. THEORETICAL MODEL OF LAMB'S WAVES PROPAGATION IN MULTILAYERED MATERIALS

Let us consider the composite layered material, which is shown in Fig. 1. It is assumed that the analyzed medium consists of n orthotropic layers. Mechanical properties of each layer are described in local coordinate system (x'_1, x'_2, x'_3) . It is worth stressing here that the origin of the local coordinate system is chosen to coincide with the top surface of the particular layer, what is shown in Fig 2. The thickness of k -th layer is equal to d_k . The particular layers are stacked normal to the x_3 axis of the global coordinate system. Thus, the plane of each layer is parallel to the (x_1, x_2) one of the global coordinate system. The wave is allowed to travel on arbitrary incident angle θ , which is measured with respect to the direction normal to the (x_1, x_2) plane, and along any angle φ . The angle φ is shown in Fig. 2. The theoretical model is formulated according to the following assumptions (Giurgiutiu, 2008; Lowe, 1995; Pant et al., 2014):

1. All layers are perfectly bonded at their interfaces.
2. The wave propagates along the $x_1 - x_3$ direction of the global coordinate system. Hence, the mechanical properties of each layer, which are defined in the local coordinate system have to be transformed to the global coordinate system
3. In each monoclinic layer there are six partial waves, namely $(+P, -P)$, $(+SV, -SV)$ and $(+SH, -SH)$ representing quasi - longitudinal (symmetric), quasi shear vertical and quasi - shear horizontal waves, respectively. The waves with plus sign are arriving from above of the interface of particular layer and the waves with the minus sign are leaving the interface.
4. The Snell's law requires that all interacting particular waves

must share the same frequency ω and spatial properties in x_1 direction at each interface. It results that in all equations, which describe the components of displacement and stress, there are the same circular frequency ω and k_1 component of the wave vector. The k_1 is the projection of the wave vector of the bulk wave onto the interface

5. The analyzed composite material is surrounded by vacuum. In other words, it is assumed that the traveling wave doesn't interact with the external environment. Hence, on the top and bottom surface of the composite material the following components of stress are equal to 0: $\sigma_{i,3} = 0, i=1,2,3$.

Most methods for solving the propagation of Lamb waves in an anisotropic medium are based on the partial wave technique. In this approach the superposition of the three upward and downward propagating waves are assumed. Taking under consideration the above assumptions, the formal solution for displacement can be proposed as follows (Hawwa, Nayfeh, 1995):

$$(u_1, u_2, u_3) = (U_1, U_2, U_3) e^{i\xi(x_1 \sin\theta + \alpha x_3 - ct)} \quad (1)$$

where u_j are the components of displacement, U_i are the amplitudes of u_j . ξ denotes the wave number, α is the unknown parameter (its value will be determined later) and c, t are the phase velocity and time, respectively. For the sake of simplicity, in the further discussion the θ angle is set to be equal to $\theta = 90^\circ$.

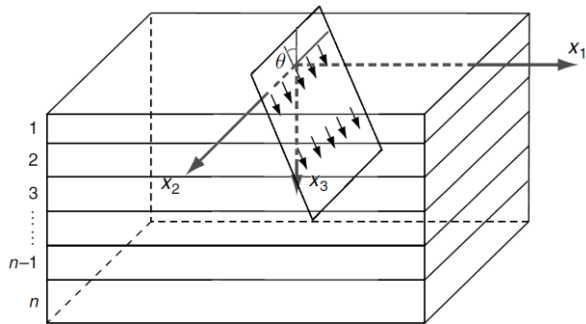


Fig. 1. Composite material with a plane wave propagating in $x_1 - x_3$ direction (Giurgiutiu, 2008)

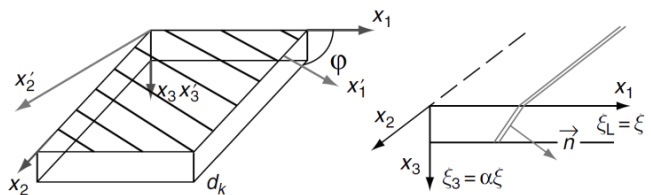


Fig. 2. The k -th layered of thickness d_k with local and global coordinate system (Giurgiutiu, 2008)

3. ELASTIC WAVES PROPAGATION IN SINGLE MONOCLINIC LAYER

According to Giurgiutiu (2008), it is assumed that the relationship between stress components and strain components in the case of single monoclinic layer of thickness d_k can be written as follows:

$$\begin{Bmatrix} \sigma_{11} \\ \sigma_{22} \\ \sigma_{33} \\ \sigma_{23} \\ \sigma_{13} \\ \sigma_{12} \end{Bmatrix} = \begin{bmatrix} C_{11} & C_{12} & C_{13} & 0 & 0 & C_{16} \\ C_{12} & C_{22} & C_{23} & 0 & 0 & C_{26} \\ C_{13} & C_{23} & C_{33} & 0 & 0 & C_{36} \\ 0 & 0 & 0 & C_{44} & C_{45} & 0 \\ 0 & 0 & 0 & C_{45} & C_{55} & 0 \\ C_{16} & C_{26} & C_{36} & 0 & 0 & C_{66} \end{bmatrix} \begin{Bmatrix} \varepsilon_{11} \\ \varepsilon_{22} \\ \varepsilon_{33} \\ \varepsilon_{23} \\ \varepsilon_{13} \\ \varepsilon_{12} \end{Bmatrix}. \quad (2)$$

Note that the above relation is defined in the global coordinate system (Fig. 1). Next, the linear relationships between the components of displacement and components of strain are given by:

$$\begin{aligned} \varepsilon_{11} &= \frac{\partial u_1}{\partial x_1}, & \varepsilon_{22} &= \frac{\partial u_2}{\partial x_2}, & \varepsilon_{33} &= \frac{\partial u_3}{\partial x_3} \\ \varepsilon_{23} &= \frac{\partial u_2}{\partial x_3} + \frac{\partial u_3}{\partial x_2}, & \varepsilon_{13} &= \frac{\partial u_1}{\partial x_3} + \frac{\partial u_3}{\partial x_1}, \end{aligned} \quad (3)$$

Combining the equations (2), (3) and (4), the system of three coupled equations is obtained, namely:

$$\begin{aligned} C_{11} \frac{\partial^2 u_1}{\partial x_1^2} + C_{66} \frac{\partial^2 u_1}{\partial x_2^2} + C_{55} \frac{\partial^2 u_1}{\partial x_3^2} + 2C_{16} \frac{\partial^2 u_1}{\partial x_1 \partial x_2} + C_{16} \frac{\partial^2 u_2}{\partial x_1^2} + C_{26} \frac{\partial^2 u_2}{\partial x_2^2} + C_{45} \frac{\partial^2 u_2}{\partial x_3^2} + (C_{12} + C_{66}) \frac{\partial^2 u_2}{\partial x_1 \partial x_2} + (C_{13} + C_{55}) \frac{\partial^2 u_3}{\partial x_1 \partial x_3} \\ + (C_{36} + C_{45}) \frac{\partial^2 u_3}{\partial x_2 \partial x_3} = \rho \frac{\partial^2 u_1}{\partial t^2} \\ C_{16} \frac{\partial^2 u_1}{\partial x_1^2} + C_{26} \frac{\partial^2 u_1}{\partial x_2^2} + C_{45} \frac{\partial^2 u_1}{\partial x_3^2} + (C_{12} + C_{66}) \frac{\partial^2 u_1}{\partial x_1 \partial x_2} + C_{66} \frac{\partial^2 u_2}{\partial x_1^2} + C_{22} \frac{\partial^2 u_2}{\partial x_2^2} + C_{44} \frac{\partial^2 u_2}{\partial x_3^2} + 2C_{26} \frac{\partial^2 u_2}{\partial x_1 \partial x_2} + (C_{36} + C_{45}) \frac{\partial^2 u_3}{\partial x_1 \partial x_3} \\ + (C_{23} + C_{44}) \frac{\partial^2 u_3}{\partial x_2 \partial x_3} = \rho \frac{\partial^2 u_2}{\partial t^2} \\ (C_{13} + C_{55}) \frac{\partial^2 u_1}{\partial x_1 \partial x_3} + (C_{36} + C_{45}) \frac{\partial^2 u_1}{\partial x_2 \partial x_3} + (C_{36} + C_{45}) \frac{\partial^2 u_2}{\partial x_1 \partial x_3} + (C_{23} + C_{44}) \frac{\partial^2 u_2}{\partial x_2 \partial x_3} + C_{55} \frac{\partial^2 u_3}{\partial x_1^2} + C_{44} \frac{\partial^2 u_3}{\partial x_2^2} + C_{33} \frac{\partial^2 u_3}{\partial x_3^2} \\ + 2C_{45} \frac{\partial^2 u_3}{\partial x_1 \partial x_2} = \rho \frac{\partial^2 u_3}{\partial t^2} \end{aligned} \quad (5)$$

Substituting the relationship (1) into (5) the system of three linear equations is obtained, namely:

$$\begin{bmatrix} C_{11} - \rho c^2 + C_{55} \alpha^2 & C_{16} + C_{45} \alpha^2 & (C_{13} + C_{55}) \alpha \\ C_{16} + C_{45} \alpha^2 & C_{66} - \rho c^2 + C_{44} \alpha^2 & (C_{36} + C_{45}) \alpha \\ (C_{13} + C_{55}) \alpha & (C_{36} + C_{45}) \alpha & C_{55} - \rho c^2 + C_{33} \alpha^2 \end{bmatrix} \begin{Bmatrix} U_1 \\ U_2 \\ U_3 \end{Bmatrix} = \begin{Bmatrix} 0 \\ 0 \\ 0 \end{Bmatrix} \quad (6)$$

In order to obtain the nontrivial solution of (6) the determinant of coefficient matrix has to be equal 0. It results in a sixth degree polynomial equation, namely:

$$A\alpha^6 + B\alpha^4 + C\alpha^2 + D = 0. \quad (7)$$

There are six real or complex roots of this equation, namely $\alpha_1 = -\alpha_2$, $\alpha_3 = -\alpha_4$ and $\alpha_5 = -\alpha_6$. Now, the components of displacement and stress can be written as follows:

$$(u_1, u_2, u_3) = \sum_{j=1}^6 (1, V_j, W_j) U_{1j} e^{i\xi(x_1 + \alpha_j x_3 - ct)}, \quad (8)$$

$$(\sigma_{33}, \sigma_{13}, \sigma_{23}) = \sum_{j=1}^6 i\xi (D_{1j}, D_{2j}, D_{3j}) U_{1j} e^{i\xi(x_1 + \alpha_j x_3 - ct)} \quad (9)$$

The elements $K_{ik}(\alpha_j)$, $i, k = 1, 2, 3$ in Eq. (11) are the components of square matrix in relationship (6). Finally, relations (8), (9), (10) and (1) can be written in the matrix form:

$$\begin{Bmatrix} u_1 \\ u_2 \\ u_3 \\ \sigma_{33} \\ \sigma_{13} \\ \sigma_{23} \end{Bmatrix} = \begin{bmatrix} 1 & 1 & 1 & 1 & 1 & 1 \\ V_1 & V_1 & V_3 & V_3 & V_5 & V_5 \\ W_1 & -W_1 & W_3 & -W_3 & W_5 & -W_5 \\ D_{11} & D_{11} & D_{13} & D_{13} & D_{15} & D_{15} \\ D_{21} & -D_{21} & D_{23} & -D_{23} & D_{25} & -D_{25} \\ D_{31} & -D_{31} & D_{33} & -D_{33} & D_{35} & -D_{35} \end{bmatrix} \begin{bmatrix} e^{i\xi\alpha_1 x_3} & 0 & 0 & 0 & 0 & 0 \\ 0 & e^{i\xi\alpha_2 x_3} & 0 & 0 & 0 & 0 \\ 0 & 0 & e^{i\xi\alpha_3 x_3} & 0 & 0 & 0 \\ 0 & 0 & 0 & e^{i\xi\alpha_4 x_3} & 0 & 0 \\ 0 & 0 & 0 & 0 & e^{i\xi\alpha_5 x_3} & 0 \\ 0 & 0 & 0 & 0 & 0 & e^{i\xi\alpha_6 x_3} \end{bmatrix} \begin{Bmatrix} U_{11} e^{i\xi(x_1 - ct)} \\ U_{12} e^{i\xi(x_1 - ct)} \\ U_{13} e^{i\xi(x_1 - ct)} \\ U_{14} e^{i\xi(x_1 - ct)} \\ U_{15} e^{i\xi(x_1 - ct)} \\ U_{16} e^{i\xi(x_1 - ct)} \end{Bmatrix} \quad (12)$$

$$\varepsilon_{12} = \frac{\partial u_1}{\partial x_2} + \frac{\partial u_2}{\partial x_1}$$

Finally, the equations of motion take the following form:

$$\begin{aligned} \frac{\partial \sigma_{11}}{\partial x_1} + \frac{\partial \sigma_{12}}{\partial x_2} + \frac{\partial \sigma_{13}}{\partial x_3} &= \rho \frac{\partial^2 u_1}{\partial t^2}, \\ \frac{\partial \sigma_{21}}{\partial x_1} + \frac{\partial \sigma_{22}}{\partial x_2} + \frac{\partial \sigma_{23}}{\partial x_3} &= \rho \frac{\partial^2 u_2}{\partial t^2}, \\ \frac{\partial \sigma_{13}}{\partial x_1} + \frac{\partial \sigma_{23}}{\partial x_2} + \frac{\partial \sigma_{33}}{\partial x_3} &= \rho \frac{\partial^2 u_3}{\partial t^2}. \end{aligned} \quad (4)$$

4. STIFFNESS MATRIX METHOD

In order to avoid any numerical instabilities, which are the main disadvantages of the transfer matrix method, Kausel (1986), Wang and Rokhlin (2001) introduced the stiffness matrix method. Generally, SMM can be written as:

$$\begin{Bmatrix} \{\sigma\}_{k-1} \\ \{\sigma\}_k \end{Bmatrix} = [K]_k = [A]_k [B]_k^{-1} = \begin{bmatrix} [D]^- & [D]^+ [H]^+ \\ [D]^- [H]^- & [D]^+ \end{bmatrix} \begin{bmatrix} [P_S]^- & [P_S]^+ [H]^+ \\ [P_S]^- [H]^- & [P_S]^+ \end{bmatrix}^{-1} \begin{Bmatrix} \{u\}_{k-1} \\ \{u\}_k \end{Bmatrix} \quad (13)$$

where subscript 'k-1' means the top surface of the k-th layer and subscript k means the bottom surface of the k-th layer. Matrices $[D]^-$, $[D]^+$ contain the coefficients associated with stresses and matrices $[P_S]^-$, $[P_S]^+$ represent the coefficients associated with displacements. These coefficients are described by relations (10) and (11). $[H]$ denotes the diagonal matrix elements in equation (12). Finally, the matrices $[A]$ and $[B]$ take the following forms (Kamal and Giurgiutiu, 2014):

$$[A]_k = \begin{bmatrix} D_{11} & D_{13} & D_{15} & D_{11} e^{i\xi\alpha_1 d_k} & D_{13} e^{i\xi\alpha_3 d_k} & D_{15} e^{i\xi\alpha_5 d_k} \\ D_{21} & D_{23} & D_{25} & -D_{21} e^{i\xi\alpha_1 d_k} & -D_{23} e^{i\xi\alpha_3 d_k} & -D_{25} e^{i\xi\alpha_5 d_k} \\ D_{31} & D_{33} & D_{35} & -D_{31} e^{i\xi\alpha_1 d_k} & -D_{33} e^{i\xi\alpha_3 d_k} & -D_{35} e^{i\xi\alpha_5 d_k} \\ D_{11} e^{i\xi\alpha_1 d_k} & D_{13} e^{i\xi\alpha_3 d_k} & D_{15} e^{i\xi\alpha_5 d_k} & D_{11} & D_{13} & D_{15} \\ D_{21} e^{i\xi\alpha_1 d_k} & D_{23} e^{i\xi\alpha_3 d_k} & D_{25} e^{i\xi\alpha_5 d_k} & D_{21} & D_{23} & D_{25} \\ D_{31} e^{i\xi\alpha_1 d_k} & D_{33} e^{i\xi\alpha_3 d_k} & D_{35} e^{i\xi\alpha_5 d_k} & D_{31} & D_{33} & D_{35} \end{bmatrix} \quad (14)$$

$$[B]_k = \begin{bmatrix} 1 & 1 & 1 & e^{i\xi\alpha_1 d_k} & e^{i\xi\alpha_3 d_k} & e^{i\xi\alpha_5 d_k} \\ V_1 & V_3 & V_5 & V_1 e^{i\xi\alpha_1 d_k} & V_3 e^{i\xi\alpha_3 d_k} & V_5 e^{i\xi\alpha_5 d_k} \\ W_1 & W_3 & W_5 & -W_1 e^{i\xi\alpha_1 d_k} & -W_3 e^{i\xi\alpha_3 d_k} & -W_5 e^{i\xi\alpha_5 d_k} \\ e^{i\xi\alpha_1 d_k} & e^{i\xi\alpha_3 d_k} & e^{i\xi\alpha_5 d_k} & 1 & 1 & 1 \\ V_1 e^{i\xi\alpha_1 d_k} & V_3 e^{i\xi\alpha_3 d_k} & V_5 e^{i\xi\alpha_5 d_k} & V_1 & V_3 & V_5 \\ W_1 e^{i\xi\alpha_1 d_k} & W_3 e^{i\xi\alpha_3 d_k} & W_5 e^{i\xi\alpha_5 d_k} & -W_1 & -W_3 & -W_5 \end{bmatrix} \quad (15)$$

In order to obtain the stiffness matrix for the whole composite material, an advanced recursive algorithm has to be applied (Rokhlin and Wang, 2002a). Let us consider two adjoining layers (1, 2), namely:

$$\begin{Bmatrix} \{\sigma\}_0 \\ \{\sigma\}_1 \end{Bmatrix} = \begin{bmatrix} [K]_{11}^A & [K]_{12}^A \\ [K]_{21}^A & [K]_{22}^A \end{bmatrix} \begin{Bmatrix} \{u\}_0 \\ \{u\}_1 \end{Bmatrix}, \quad \begin{Bmatrix} \{\sigma\}_1 \\ \{\sigma\}_2 \end{Bmatrix} = \begin{bmatrix} [K]_{11}^B & [K]_{12}^B \\ [K]_{21}^B & [K]_{22}^B \end{bmatrix} \begin{Bmatrix} \{u\}_1 \\ \{u\}_2 \end{Bmatrix} \quad (16)$$

where subscripts denote the interfaces. By excluding $\{\sigma\}_1$ and $\{u\}_1$ from the first relation and substituting in the second one, the matrix, which relates $\{\sigma\}_0$ $\{u\}_0$ to $\{\sigma\}_2$ $\{u\}_2$, is obtained. This combined matrix is a stiffness matrix for these two bonded layers, namely:

$$\begin{Bmatrix} \{\sigma\}_0 \\ \{\sigma\}_2 \end{Bmatrix} = \begin{bmatrix} [K]_{11}^A + [K]_{12}^A ([K]_{11}^B - [K]_{22}^A)^{-1} [K]_{21}^A & -[K]_{12}^A ([K]_{11}^B - [K]_{22}^A)^{-1} [K]_{12}^B \\ [K]_{21}^B - [K]_{21}^A ([K]_{11}^B - [K]_{22}^A)^{-1} [K]_{12}^B & [K]_{22}^B - [K]_{21}^A ([K]_{11}^B - [K]_{22}^A)^{-1} [K]_{12}^B \end{bmatrix} \begin{Bmatrix} \{u\}_0 \\ \{u\}_2 \end{Bmatrix} \quad (17)$$

Denoting the stiffness matrix obtained by $[K]^A$ and the stiffness matrix for the third layer by $[K]^B$, we can recursively apply the relation (17) to obtain the global stiffness matrix, which relates the stresses to the displacements for the top and bottom surface of the whole composite plate. The wave characteristic equation for the whole composite structure is obtained from the total stiffness matrix. Assuming that the components of stress on the top and bottom surface equal zero, in order to find the solution of (17), the determinant of the matrix 6x6 has to be computed.

5. NUMERICAL EXAMPLES

The dispersion curves are determined for three different plates. The first plate consists of one layer, which is made of carbon fiber/epoxy resin, namely CFRP, Fibers T300, Matrix N5208. The total thickness of the plate is equal to $d = 2$ mm. The next plate consists of 8 layers with following stacking sequence $[0^\circ, 90^\circ, 0^\circ, 90^\circ, 0^\circ, 90^\circ, 0^\circ, 90^\circ]$. Each layer is made of identical material, namely carbon fiber/epoxy resin. The layers have also identical thickness $d_k = 0.25$ mm. Thus the total thickness of composite material is equal to $d = 2$ mm. The last plate is a hybrid composite, where the layers are as follows: $[Al, 90^\circ, 0^\circ, 90^\circ, 0^\circ, 90^\circ, 0^\circ]$.

Al denotes aluminum alloy PA38 and the rest of layers are made of carbon fibers/epoxy resin. The thickness of aluminum alloy layer is equal to $d_1=0.5$ mm. The rest layers have identical thickness $d_k = 0.25$ mm. The total thickness of the plate is also equal to $d = 2$ mm. The material properties of the aluminum alloy PA38 are: $E = 69.5$ GPa, $\nu = 0.33$ and density $\rho = 2700$ kg/m³ and carbon fibers/epoxy resin lamina are: $E_1 = 181$ GPa, $E_2 = 10.3$ GPa, $G_{12} = 7.17$ GPa, $\nu_{12} = 0.28$ and density $\rho = 1.6$ kg/m³. It is worth stressing here that the carbon layers are strongly orthotropic. It could cause some difficulties in numerical calculation. In order to find the solution of the studied problem an appropriate computer program is developed with the aid of SCILAB free software. In order to find the solution of the wave characteristic equation the bisection method is applied.

5.1. Single Lamina

In Fig. 3 there are shown the wave dispersion curves (phase and group velocities) obtained for a single lamina, where the waves propagate along the material principle direction x_1 , $\varphi = 0^\circ$ (Fig. 1). In these figures the fundamental symmetric P_0 , shear vertical SV_0 and shear horizontal SH_0 modes are highlighted.

Additionally, the four higher modes are present in the considered range of frequency. Unfortunately, the applied method does not allow the full identification of what kind of wave mods are. From the practical point of view the most important are the fundamental ones, namely P_0 , SV_0 , SH_0 . The highest phase velocity is observed in the case of symmetric mod P_0 , $c \approx 10660$ m/s. Moreover, its phase velocity is almost constant while the frequency is less than 500 kHz. For the greater frequency the significant change is observed. The SH_0 mod is constant in the whole studied range of frequency. To the contrary of the P_0 and SH_0 modes, the SV_0 one is strongly dispersive for the relatively small values of frequency. For frequency $f = 400$ kHz the phase velocity of this mode is also almost constant. It is worth noting that the all fundamental modes are convergent to the phase velocity equal to $c \approx$

2000 m/s. Thus in the experiment for the sufficiently large frequency of the excited signal, the identification of these modes could be very difficult

In the Fig. 4 there are depicted the characteristic dispersion curves for the elastic waves, which travels in the direction which is perpendicular to the x_1 material principal direction, $\varphi = 90^\circ$. Now the initial phase velocity of the P_0 symmetric fundamental mode is significantly smaller $c \approx 2540$ m/s due to the reduced stiffness of the lamina in this direction ($E_2=10.5$ GPa). The maximum value of the phase velocity in the case of the SV_0 mode is also reduced. The phase velocity of SH_0 mode is constant and identical as before. It is worth noting here that the number of higher modes is also changed. Now the seven higher modes are present in the considered range of frequency.

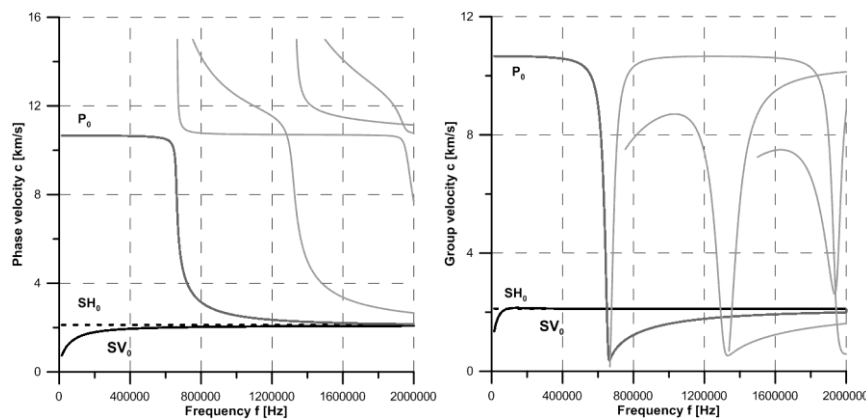


Fig. 3. Phase and group velocities. Single lamina, angle of waves propagation $\varphi=0^\circ$

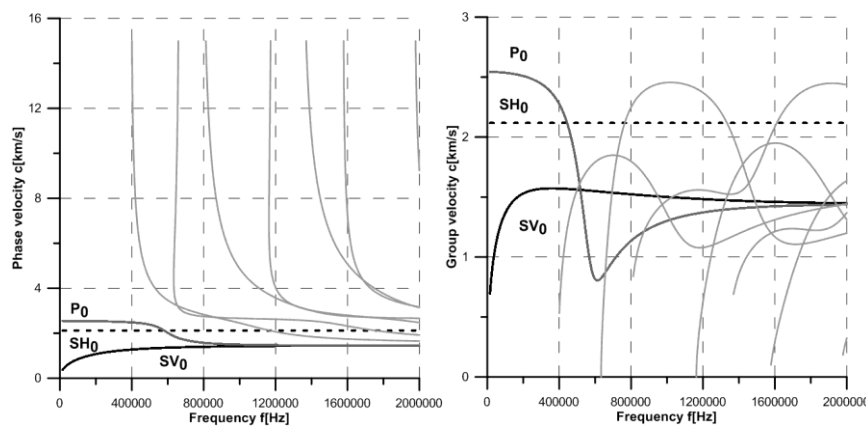


Fig. 4. Phase and group velocities. Single lamina, angle of waves propagation $\varphi=90^\circ$

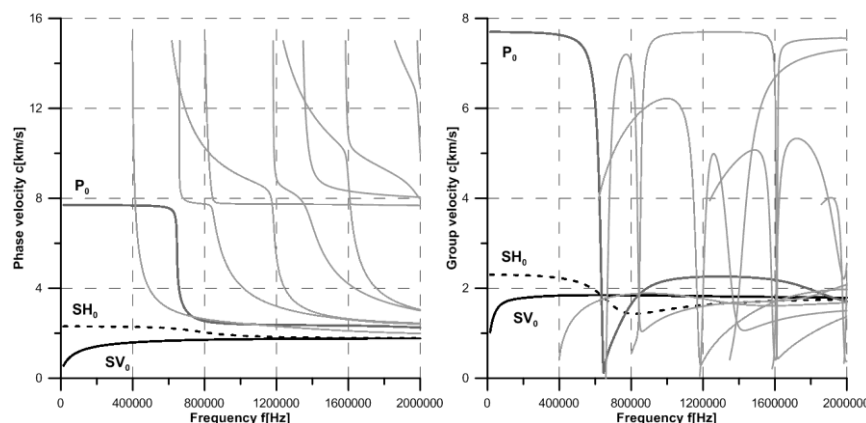


Fig. 5. Phase and group velocities. Single lamina, angle of waves propagation $\varphi=45^\circ$

However quite different dispersion curves are obtained in the case of waves propagation angle $\varphi = 45^\circ$, what is depicted in the Fig. 5. The initial (low frequency) phase velocity of the fundamental symmetric mode P_0 is equal to $c \approx 7700$ m/s. Moreover, for frequency $f \approx 500$ kHz as well as in the previous cases, the sudden change of the phase and group velocity is observed. The shear horizontal mode SH_0 is not constant any more. The slight variation is also observed. The initial SH_0 phase velocity is equal to $c \approx 2300$ m/s. The shear vertical SV_0 is strongly dispersive for the low values of frequency. For the higher frequencies, great then $f > 1.2$ MHz the phase velocity of this mode is almost identical in comparison with SH_0 one. The most significant difference is observed in number of higher modes. Now ten higher modes are present. The first of them appears for the frequency equal to $f \approx 4$

kHz. It is relatively low value of frequency in comparison with the previous cases. Finally, in Fig. 6 there are presented the relationships between the fundamental modes P_0 , SH_0 and SV_0 and the waves propagation angle φ . These graphs are created for the fixed value of frequency $f = 250$ kHz. According to the authors of this work, the frequency equal to $f = 250$ kHz of the excitation signal is the most reasonable value from the practical point of view. The strongest dependency is observed in case of the symmetric mode P_0 . The shear modes are not so sensitive on the wave propagation angle φ . It is worth noting that the SH_0 mode is almost insensitive on the angle φ . Moreover, the values of the phase and group velocities for assumed frequency are very similar.

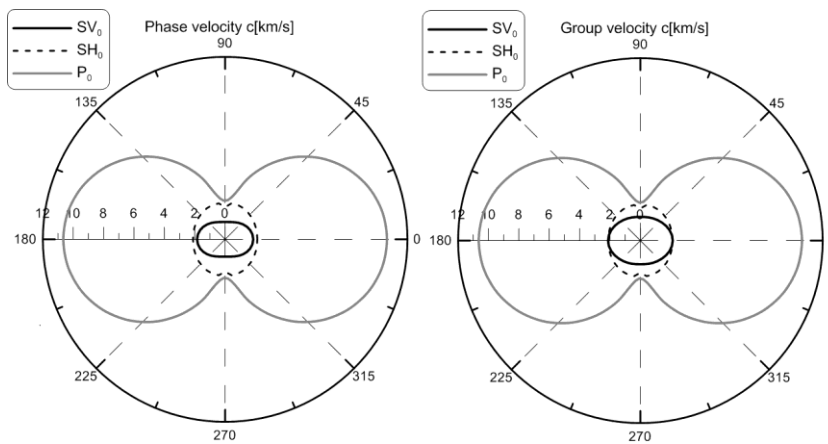


Fig. 6. Phase and group velocities with respect to angle of wave propagation. Fixed frequency $f = 250$ kHz.

5.2. Layered composite $[0^\circ, 90^\circ, 0^\circ, 90^\circ, 0^\circ, 90^\circ, 0^\circ, 90^\circ]$

In the case of the layered composite, when the waves propagation angle $\varphi = 0^\circ$, the fundamental symmetric mode P_0 has initial phase velocity $c = 7750$ m/s. It is worth noting that this value is smaller in comparison with the initial phase velocity obtained in the case of single lamina. In contrast to the previously discussed cases, now this mode is slight dispersive in the initial range of frequency. For the frequency value $f \approx 500$ kHz the sudden

change is observed. Similar effect has been described in the case of a single lamina. For the frequency $f > 1.2$ MHz the mode P_0 is almost constant. The shear horizontal SH_0 mode is constant in the whole investigated range of frequency. Its phase velocity is equal to $c = 2120$ m/s. The shear vertical SV_0 mode is very similar to those, which are obtained for the single lamina. Additionally, seven higher modes are observed in the studied range of frequency. It should be stressed here that for the waves propagation angle $\varphi = 90^\circ$, the obtained results are identical.

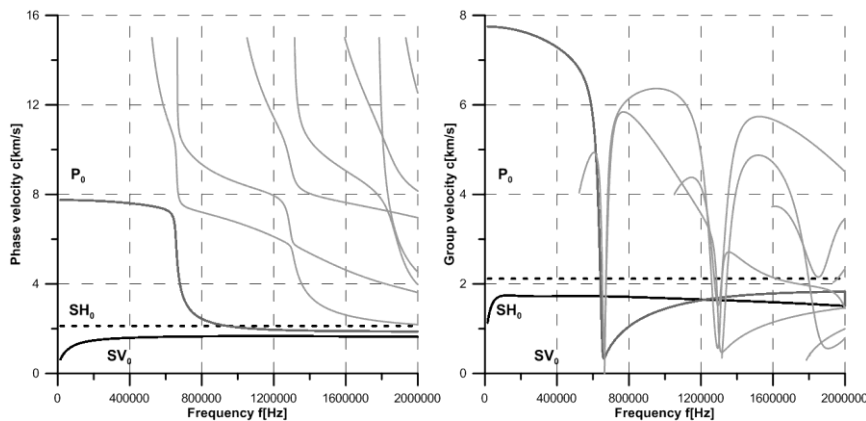


Fig. 7. Phase and group velocities. Layered composite $[0^\circ, 90^\circ, 0^\circ, 90^\circ, 0^\circ, 90^\circ, 0^\circ, 90^\circ]$. Angle of waves propagation $\varphi = 0^\circ, 90^\circ$

For the waves propagation angle $\varphi = 45^\circ$, the obtained dispersion curves in the case of P_0 and SV_0 modes are similar to

those, which are presented in the previous cases, what is depicted in Fig. 8. The initial phase velocity for P_0 mod is equal to $c =$

5950 m/s. However, behavior of the fundamental shear horizontal mode SH_0 is qualitatively different. It is rather similar to the P_0 mode. Additionally, its initial velocity $c = 5400$ m/s. For the frequency $f > 1.2$ MHz the sudden drop is visible, what remains the fundamental symmetric mode P_0 with frequency $f > 500$ kHz. It is also characteristic in the case of group velocities of modes P_0 and SH_0 . The number of higher modes increases and now it is equal to eight. The shapes of the higher modes dispersion curves are also substantially different in comparison with those, which are presented in Fig. 7.

The phase and group velocities for the fixed frequency $f = 250$ kHz are presented in Fig. 9. It should be stressed here that the

these graphs are also substantially different in comparison with those which are presented in Fig. 6. The shear vertical mode SV_0 seems to be insensitive on the waves propagation angle φ . The symmetric mode P_0 varies not significantly with respect to this parameter. However the phase and group velocity of the shear horizontal mode SH_0 strongly depends on the angle φ . For the values of the angle φ equal to 45° , 135° , 225° and 315° the discussed velocities have the highest values. The maximal value of the phase velocity is over two times larger in comparison with the minimal one.

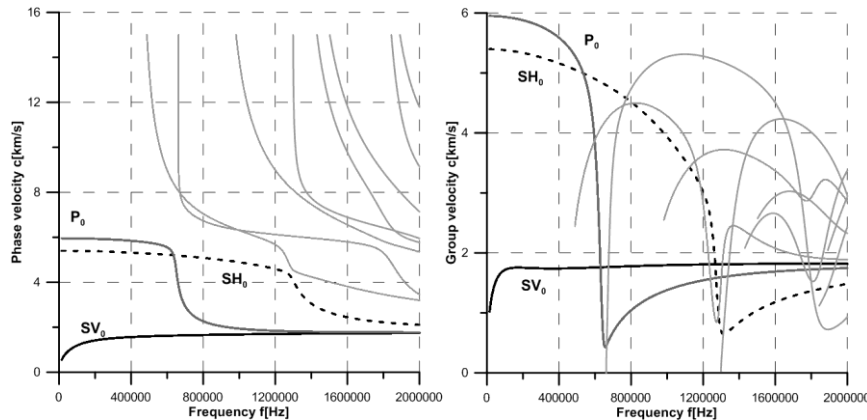


Fig. 8. Phase and group velocities. Layered composite $[0^\circ, 90^\circ, 0^\circ, 90^\circ, 0^\circ, 90^\circ, 0^\circ, 90^\circ]$. Angle of waves propagation $\varphi = 45^\circ$

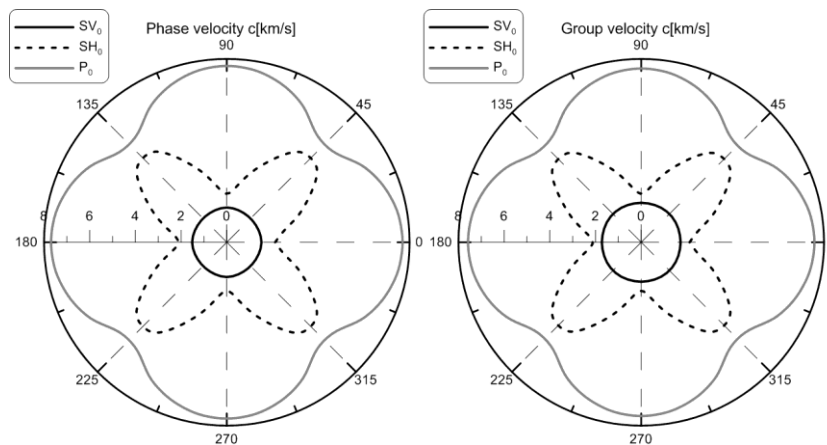


Fig. 9. Phase and group velocities with respect to angle of wave propagation. Fixed frequency $f = 250$ kHz. Layered composite $[0^\circ, 90^\circ, 0^\circ, 90^\circ, 0^\circ, 90^\circ, 0^\circ, 90^\circ]$

5.3. Hybrid composite $[Al, 90^\circ, 0^\circ, 90^\circ, 0^\circ, 90^\circ, 0^\circ]$

It should be stressed here that in the previously presented cases there has been no any numerical instabilities and the reliable numerical solution of the wave characteristic equation can be always obtained. Unfortunately, in the case of hybrid composite the dispersion curves are determined only for the waves propagation angle $\varphi = 0^\circ$. In the case of the other values of φ the problems are met even in estimation of the fundamental modes SH_0 and P_0 . According to the authors experience it could be caused by the fact that these modes are very close to each other and it is impossible to extract them. Additionally, there is a significant difference between the Young's modulus of the aluminum alloy and carbon fibers. This difference could cause some disturbances

with propagation of elastic waves through the interface of aluminum layer and carbon fiber layer.

In Fig. 10 there is presented the dispersion curves. These curves are computed for the waves propagation angle $\varphi = 0^\circ$. Generally, the obtained curves are similar to those which are presented above. The initial value of the phase velocity of the symmetric mode P_0 is equal to $c = 6990$ m/s. The shear horizontal mode SH_0 slightly varies with respect to the frequency. However, the group velocity of this mode for frequency equal to $f = 1.48$ MHz suddenly changes. The shear vertical mode SV_0 is very regular and it remains the curves, which are presented above. Besides, there are nine higher modes. To the contrary to previously presented cases, now it possible to identify the higher shear horizontal modes, namely from SH_1 to SH_4 .

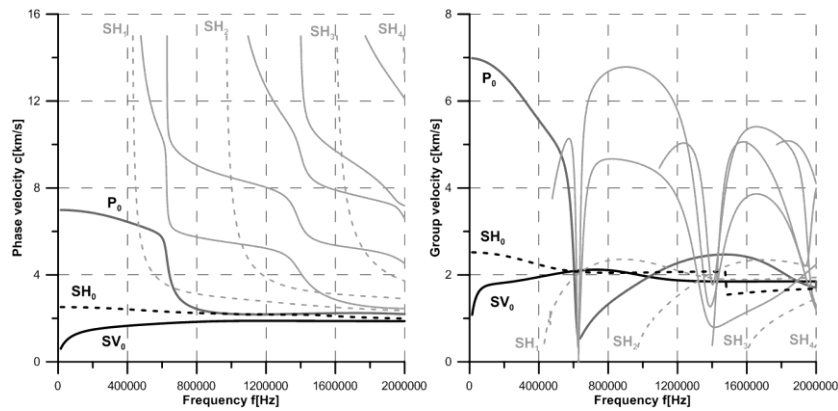


Fig. 10. Phase and group velocities. Hybrid composite [Al, 90°, 0°, 90°, 0°, 90°, 0°]. Angle of waves propagation $\varphi = 0^\circ$

6. CONCLUSIONS

In the present work the dispersion curves are estimated for a different composite materials, namely: single lamina, multilayered composite with quasi - isotropic mechanical properties and hybrid composite material. In the case of single lamina and quasi - isotropic composite all layers are made of carbon fiber/epoxy resin. In the latter case, the investigated material consists of carbon fiber/epoxy resin and single layer, which is made of aluminum alloy Pa38. The main conclusion is that if the all layers of studied composite are made of identical material, the stiffness matrix approach in an effective tool for determining the dispersion curves. It is relatively simple and easy to use in comparison with other method, like transfer matrix method or global matrix method. However, if the composite contains the layers, which are made of different materials, the obtaining of dispersion curves could be very difficult or even impossible. According to the authors experience, this effect is caused by the significant difference between the mechanical properties of the layers (the values of Young's modulus). Generally, the shape and the number of elastic wave modes, which are present in the investigated range of frequency, strictly depends on the mechanical properties of the whole composite structure as well as on the waves propagation angle φ . For the angle φ different than 0° and 90° , the number of higher modes is the largest. Qualitatively, the behavior of the fundamental modes are similar in all investigated cases. For the low frequency the highest phase and group velocity has always the symmetric mode P_0 .

REFERENCES

1. Barski M., Pająk P. (2016), An application of stiffness matrix method to determining of dispersion curves for arbitrary composite materials, *Journal of KONES Powertrain and Transport*, 23(1), 47-54.
2. Giurgiutiu V. (2008), *Structural Health Monitoring with Piezoelectric Wafer Active Sensors*, Elsevier.
3. Haskell N.A. (1953), Dispersion of surface waves on multilayer-media, *Bulletin of the Seismological Society of America*, 43, 17- 34.
4. Hawwa M.A., Nayfeh H.A. (1995), The general problem of thermoelastic waves in anisotropic periodically laminated composites, *Composite Engineering*, 5, 1499- 1517.
5. Kamal A., Giurgiutiu V. (2014), Stiffness Transfer Matrix Method (STMM) for Stable Dispersion Curves Solution in Anisotropic Composites, *Proc. of SPIE*, Vol. 9064.
6. Kausel E. (1986), Wave propagation in anisotropic layered media. *International Journal for Numerical Methods in Engineering*, 23, 1567-1578.
7. Knopoff L. (1964), A matrix method for elastic waves problems. *Bulletin of the Seismological Society of America*, 43, 431-438.
8. Lowe J.S.M. (1995), Techniques for Modeling Ultrasonic Waves in Multilayered Media, *IEEE Transactions on Ultrasonics, Ferroelectric and Frequency Control*, 42, 525-542.
9. Nayfeh A.H. (1991), The general problem of elastic wave propagation in multilayered anisotropic media, *Journal of the Acoustic. Society of America*, 89, 1521- 1531.
10. Pant S., Laliberte J., Martinez M, Rocha B. (2014), Derivation and experimental validation of Lamb wave equations for an n - layered anisotropic composite laminate, *Composite Structure*, 111, 566-579.
11. Pavlakovic B., Lowe M. (2003), *DISPERSE Manual*, Imperial College, London.
12. Press F., Harkrider D., Seafeldt C.A. (1961), A fast convenient program for computations of surface - wave dispersion curves in multilayered media, *Bulletin of the Seismological Society of America*, 51, 495- 502.
13. Randall M.J. (1967), Fast programs for layered half - space problems, *Bulletin of the Seismological Society of America*, 57, 1299-1316.
14. Rokhlin S.I., Wang L. (2002a), Stable recursive algorithm for elastic wave propagation in layered anisotropic media: Stiffness matrix method, *Journal of the Acoustic Society of America*, 112, 822-834.
15. Rokhlin S.I., Wang L. (2002b), Ultrasonic waves in layered anisotropic media: characterization of multidirectional composites, *International Journal of Solids & Structures*, 39, 5529- 5545.
16. Royer D., Dieulesaint E. (2000), *Elastic Waves in Solids*, Springer.
17. Schmidt H., Tango G. (1986), Efficient global matrix approach to the computation of synthetic seismograms, *Geophysical Journal of Royal Astronomical Society*, 84, 331- 359.
18. Schwab F.A. (1970), Surface - wave dispersion computations: Knopoff's method, *Bulletin of the Seismological Society of America*, 60, 1491- 1520.
19. Soroohan S., Constantin N., Gavan M., Anghel V. (2011), Extraction of dispersion curves for waves propagating in free complex waveguides by standard finite element codes, *Ultrasonics*, 51, 503-515.
20. Thomson W. T. (1950), Transmission of elastic waves through a stratified solid medium. *Journal of Applied Physics*, 21, 89-93.
21. Wang L., Rokhlin S.I. (2001), Stable reformulation of transfer matrix method for wave propagation in layered anisotropic media, *Ultrasonics*, 39, 413-424.

Acknowledgement: The research project has been financed by National Science Center of Poland pursuant to the decision No. DEC-2013/09/B/ST8/00178.